Electron impact excitation of Ni-like gold studied by Dirac R-matrix method*

Fan Quan-Ping(范全平)[a)b)], Wang Wen-Hui(汪文慧)[b)], Hu Feng(胡 峰)[c)], Cao Lei-Feng(曹磊峰)[b)], Zhang Qiang-Qiang(张强强)[b)], Liu Yu-Wei(刘钰薇)[b)], and Jiang Gang(蒋 刚)[a)†]

[a)] *Institute of Atomic and Molecular Physics, Sichuan University, Chengdu* 610065, *China*
[b)] *Research Center of Laser Fusion, China Academy of Engineering Physics, Mianyang* 621900, *China*
[c)] *School of Mathematic and Physical Science, Xuzhou Institute of Technology, Xuzhou* 221400, *China*

(Received 17 March 2014; revised manuscript received 5 May 2014; published online 17 September 2014)

We calculate the electron impact excitation of Ni-like gold by using the Dirac R-matrix theory, and the corresponding collision strengths and effective collision strengths are obtained. In the calculations of the level energy, $(1s^22s^22p^6)3s^23p^63d^{10}$, $3s^23p^63d^94l$, $3s^23p^53d^{10}4l$, and $3s3p^63d^{10}4l$ ($l = 0,1,2,3$) configurations are included and 107 fine-structure levels are generated. In the calculations of the collision strengths, only the first 59 levels are included. Comparisons are made with the distorted wave (DW) results of Zeng *et al.* for both collision strengths and effective collision strengths. For the collision strengths, the two sets of calculations are in excellent agreement for most of the transitions. However, because of the inclusion of the resonances, our effective collision strengths are generally several times larger than those of Zeng *et al.*. The accuracy of our calculations is assessed.

Keywords: electron impact excitation, R-matrix method, Ni-like gold

PACS: 34.50.–s, 34.50.Fa, 34.80.Dp **DOI:** 10.1088/1674-1056/23/11/113401

1. Introduction

Gold is used as a work material of particular interest for the indirect laser drive inertial confinement fusion (ICF), in which laser radiation heats the inside of a gold hohlraum and intense X-rays are emitted by the produced gold plasma. The emitted X-rays drive the capsule implosion and influence the resulting fusion yield. Therefore, many studies[1–4] have been performed for the X-ray emission spectra of Au ions. Ions near the ionization stage of Ni-like Au are of special interest, either for dense plasmas or coronal plasmas.[5] On the other hand, since a large laser amplification is possible in the UV and X-ray region, Ni-like ions with high atomic numbers are of considerable interest in collisionally pumped X-ray lasers, among which the Ni-like Au is a useful candidate.

To the best of our knowledge, the calculations of the electron impact excitation for Ni-like Au are sparse. Xie *et al.*[6] calculated the collision strengths and the rate coefficients for the electron impact excitation of highly charged Ni-like ions ($Z = 86$–92) by using a fully relativistic distorted wave (DW) method, however, Ni-like Au was not included in their calculations. Zhang *et al.*,[7] Zeng *et al.*,[8] and Yang *et al.*[9] performed the calculations for Ni-like Au and all of them were based on the DW methods, however, the contribution of the resonances was not included. For the forbidden transitions, the contribution of the resonances is very important and could obviously influence the rate coefficients. On the other hand, for the modeling of the plasmas, results are required for all transitions among the excited levels. Therefore, our aim is to report the collision strengths Ω and the effective collision strengths γ for all transitions considered for Ni-like Au. Comparisons are made with the results of DW theories. In our Dirac atomic R-matrix code (DARC) calculations, the contributions of resonances, channel coupling, and relativity are included. However, the effects of radiation damping[10,11] are not included, which will be systematically discussed in future work.

To achieve our goal, the fully relativistic GRASP code[12] is used to generate the wavefunctions, and the Dirac atomic R-matrix code[13] is used to calculate the collision strengths. To include the contribution of the resonances, 10000 energy points in the threshold region must be calculated. The DARC calculations for every energy point are time-consuming. So parallelization is needed. The PSTGF package is combined with serial DARC to achieve the parallel calculations for every energy point. It takes 50 CPUs and five days to complete the parallel calculations.

2. Atomic structure

The $(1s^22s^22p^6)3s^23p^63d^{10}$, $3s23p^63d^94l$, $3s^23p^53d^{10}4l$, and $3s3p^63d^{10}4l$ ($l = 0,1,2,3$) configurations have been included in the GRASP calculation of Ni-like Au, which gives rise to 107 fine-structure levels in total, as listed in Table 1. The option of extended average level (EAL) has been used in our GRASP calculation, in which a weighted (proportional to $2J+1$) trace of the Hamiltonian matrix is minimized. This

*Project supported by the National Natural Science Foundation of China (Grant Nos. 11174213 and 11304266).
†Corresponding author. E-mail: gjiang@scu.edu.cn
© 2014 Chinese Physical Society and IOP Publishing Ltd

produces a compromise set of orbitals describing closely lying states with moderate accuracy.

In addition, the Breit and QED corrections are included in our energy level calculations (GRASP2), and comparisons are made with the results without Breit and QED corrections (GRASP1). From Table 1, we can see that the effects of the Breit and QED corrections are more and more important with the increase of the energy level. When the Breit correction is included, level ordering for levels 68 and 69 is changed as shown in Table 1. Comparisons with the results of Yang *et al.* and Zeng *et al.* are also made in Table 1. Our results are in excellent agreement with the results of Zeng *et al.,* the difference between the two sets of calculations is less than 0.1% for all energy levels, except for level 5, for which the difference between them is about 0.6%. Comparing with the data of Yang *et al.*, we also find that the difference of the two sets of calculations is less than 0.2% for all energy levels considered. Above all, we believe that our calculations from GRASP are probably accurate.

Table 1. State definitions and energy levels of Ni-like Au.

Level	State configuration	Level	GRASP1	GRASP2	Yang	Zeng
1	$3s^2 3p_{1/2}^2 3p_{3/2}^4 3d_{3/2}^4 3d_{5/2}^6$	$^1S_0^e$	0	0	0	0
2	$3s^2 3p_{1/2}^2 3p_{3/2}^4 3d_{3/2}^4 3d_{5/2}^5 4s$	$^3D_3^e$	1856.15	1855.53		1857.02
3	$3s^2 3p_{1/2}^2 3p_{3/2}^4 3d_{3/2}^4 3d_{5/2}^5 4s$	$^1D_2^e$	1858.16	1857.63		1859.18
4	$3s^2 3p_{1/2}^2 3p_{3/2}^4 3d_{3/2}^3 3d_{5/2}^6 4s$	$^3D_1^e$	1949.01	1946.64		1958.36
5	$3s^2 3p_{1/2}^2 3p_{3/2}^4 3d_{3/2}^3 3d_{5/2}^6 4s$	$^3D_2^e$	1950.44	1947.96	1950.61	1949.72
6	$3s^2 3p_{1/2}^2 3p_{3/2}^4 3d_{3/2}^4 3d_{5/2}^5 4p_{1/2}$	$^3P_2^o$	1965.71	1965.39		1965.83
7	$3s^2 3p_{1/2}^2 3p_{3/2}^4 3d_{3/2}^4 3d_{5/2}^5 4p_{1/2}$	$^3F_3^o$	1967.17	1966.59		1967.08
8	$3s^2 3p_{1/2}^2 3p_{3/2}^4 3d_{3/2}^3 3d_{5/2}^6 4p_{1/2}$	$^3F_2^o$	2058.85	2056.43		2057.11
9	$3s^2 3p_{1/2}^2 3p_{3/2}^4 3d_{3/2}^3 3d_{5/2}^6 4p_{1/2}$	$^3D_1^o$	2062.56	2060.29	2062.20	2061.07
10	$3s^2 3p_{1/2}^2 3p_{3/2}^4 3d_{3/2}^4 3d_{5/2}^5 4p_{3/2}$	$^3F_4^o$	2112.83	2110.62		2111.24
11	$3s^2 3p_{1/2}^2 3p_{3/2}^4 3d_{3/2}^4 3d_{5/2}^5 4p_{3/2}$	$^1D_2^o$	2114.71	2112.73		2113.37
12	$3s^2 3p_{1/2}^2 3p_{3/2}^4 3d_{3/2}^4 3d_{5/2}^5 4p_{3/2}$	$^1P_1^o$	2115.96	2113.98		2114.77
13	$3s^2 3p_{1/2}^2 3p_{3/2}^4 3d_{3/2}^4 3d_{5/2}^5 4p_{3/2}$	$^3D_3^o$	2118.32	2116.31		2117.03
14	$3s^2 3p_{1/2}^2 3p_{3/2}^4 3d_{3/2}^3 3d_{5/2}^6 4p_{3/2}$	$^3P_0^o$	2201.87	2198.20		2198.98
15	$3s^2 3p_{1/2}^2 3p_{3/2}^4 3d_{3/2}^3 3d_{5/2}^6 4p_{3/2}$	$^3P_1^o$	2206.86	2203.04		2203.91
16	$3s^2 3p_{1/2}^2 3p_{3/2}^4 3d_{3/2}^3 3d_{5/2}^6 4p_{3/2}$	$^3F_3^o$	2207.39	2203.35		2204.24
17	$3s^2 3p_{1/2}^2 3p_{3/2}^4 3d_{3/2}^3 3d_{5/2}^6 4p_{3/2}$	$^3D_2^o$	2210.14	2206.29		2207.20
18	$3s^2 3p_{1/2}^2 3p_{3/2}^4 3d_{3/2}^4 3d_{5/2}^5 4d_{3/2}$	$^3P_1^e$	2272.61	2270.33		2270.21
19	$3s^2 3p_{1/2}^2 3p_{3/2}^4 3d_{3/2}^4 3d_{5/2}^5 4d_{3/2}$	$^3G_4^e$	2278.45	2275.61		2275.63
20	$3s^2 3p_{1/2}^2 3p_{3/2}^4 3d_{3/2}^4 3d_{5/2}^5 4d_{3/2}$	$^3D_2^e$	2279.72	2277.24		2277.25
21	$3s^2 3p_{1/2}^2 3p_{3/2}^4 3d_{3/2}^4 3d_{5/2}^5 4d_{3/2}$	$^3F_3^e$	2282.39	2279.85		2279.88
22	$3s^2 3p_{1/2}^2 3p_{3/2}^4 3d_{3/2}^4 3d_{5/2}^5 4d_{5/2}$	$^1P_1^e$	2306.66	2303.26		2303.20
23	$3s^2 3p_{1/2}^2 3p_{3/2}^4 3d_{3/2}^4 3d_{5/2}^5 4d_{5/2}$	$^3G_5^e$	2308.67	2305.07		2305.06
24	$3s^2 3p_{1/2}^2 3p_{3/2}^4 3d_{3/2}^4 3d_{5/2}^5 4d_{5/2}$	$^3D_3^e$	2312.77	2309.51		2309.54
25	$3s^2 3p_{1/2}^2 3p_{3/2}^4 3d_{3/2}^4 3d_{5/2}^5 4d_{5/2}$	$^1D_2^e$	2313.91	2310.86		2310.97
26	$3s^2 3p_{1/2}^2 3p_{3/2}^4 3d_{3/2}^4 3d_{5/2}^5 4d_{5/2}$	$^3F_4^e$	2314.90	2311.60		2311.68
27	$3s^2 3p_{1/2}^2 3p_{3/2}^4 3d_{3/2}^4 3d_{5/2}^5 4d_{5/2}$	$^3P_0^e$	2333.50	2330.40		2330.50
28	$3s^2 3p_{1/2}^2 3p_{3/2}^4 3d_{3/2}^3 3d_{5/2}^6 4d_{3/2}$	$^3D_1^e$	2370.25	2365.71	2370.19	2365.92
29	$3s^2 3p_{1/2}^2 3p_{3/2}^4 3d_{3/2}^3 3d_{5/2}^6 4d_{3/2}$	$^3G_3^e$	2370.70	2366.03		2366.26
30	$3s^2 3p_{1/2}^2 3p_{3/2}^3 3d_{3/2}^4 3d_{5/2}^6 4s$	$^3P_2^o$	2374.57	2370.67		2371.44
31	$3s^2 3p_{1/2}^2 3p_{3/2}^4 3d_{3/2}^3 3d_{5/2}^6 4d_{3/2}$	$^3F_2^e$	2376.84	2372.45		2372.79
32	$3s^2 3p_{1/2}^2 3p_{3/2}^3 3d_{3/2}^4 3d_{5/2}^6 4s$	$^1P_1^o$	2378.20	2374.28		2375.17
33	$3s^2 3p_{1/2}^2 3p_{3/2}^4 3d_{3/2}^3 3d_{5/2}^6 4d_{5/2}$	$^3P_1^e$	2399.34	2394.52		2394.68
34	$3s^2 3p_{1/2}^2 3p_{3/2}^4 3d_{3/2}^3 3d_{5/2}^6 4d_{5/2}$	$^3G_4^e$	2403.35	2397.96		2398.20
35	$3s^2 3p_{1/2}^2 3p_{3/2}^4 3d_{3/2}^3 3d_{5/2}^6 4d_{5/2}$	$^3D_2^e$	2405.03	2399.97		2400.22
36	$3s^2 3p_{1/2}^2 3p_{3/2}^4 3d_{3/2}^3 3d_{5/2}^6 4d_{5/2}$	$^3F_3^e$	2407.17	2402.07		2402.34
37	$3s^2 3p_{1/2}^2 3p_{3/2}^4 3d_{3/2}^3 3d_{5/2}^6 4d_{3/2}$	$^1S_0^e$	2418.13	2414.65		2414.38
38	$3s^2 3p_{1/2}^2 3p_{3/2}^4 3d_{3/2}^4 3d_{5/2}^5 4f_{5/2}$	$^3P_0^o$	2473.22	2470.09		2469.95
39	$3s^2 3p_{1/2}^2 3p_{3/2}^4 3d_{3/2}^4 3d_{5/2}^5 4f_{5/2}$	$^3P_1^o$	2477.11	2473.60		2473.45
40	$3s^2 3p_{1/2}^2 3p_{3/2}^4 3d_{3/2}^4 3d_{5/2}^5 4f_{5/2}$	$^3H_5^o$	2482.20	2477.98		2477.77
41	$3s^2 3p_{1/2}^2 3p_{3/2}^4 3d_{3/2}^4 3d_{5/2}^5 4f_{5/2}$	$^3D_2^o$	2482.80	2479.22		2479.06
42	$3s^2 3p_{1/2}^2 3p_{3/2}^3 3d_{3/2}^4 3d_{5/2}^6 4p_{1/2}$	$^3P_1^e$	2484.90	2481.26		2480.99

Table 1. (*Continued*).

Level	State configuration	Level	GRASP1	GRASP2	Yang	Zeng
43	$3s^2 3p^2_{1/2} 3p^3_{3/2} 3d^4_{3/2} 3d^6_{5/2} 4p_{1/2}$	$^3D^e_2$	2485.96	2482.10		2481.87
44	$3s^2 3p^2_{1/2} 3p^4_{3/2} 3d^4_{3/2} 3d^5_{5/2} 4f_{5/2}$	$^3F^o_3$	2486.46	2482.68		2482.49
45	$3s^2 3p^2_{1/2} 3p^4_{3/2} 3d^4_{3/2} 3d^5_{5/2} 4f_{5/2}$	$^3G^o_4$	2487.66	2483.83		2483.61
46	$3s^2 3p^2_{1/2} 3p^4_{3/2} 3d^4_{3/2} 3d^5_{5/2} 4f_{7/2}$	$^3H^o_6$	2489.37	2484.73		2484.58
47	$3s^2 3p^2_{1/2} 3p^4_{3/2} 3d^4_{3/2} 3d^5_{5/2} 4f_{7/2}$	$^1D^o_2$	2490.47	2486.39		2486.27
48	$3s^2 3p^2_{1/2} 3p^4_{3/2} 3d^4_{3/2} 3d^5_{5/2} 4f_{7/2}$	$^3F^o_4$	2495.47	2491.20		2491.05
49	$3s^2 3p^2_{1/2} 3p^4_{3/2} 3d^4_{3/2} 3d^5_{5/2} 4f_{7/2}$	$^3G^o_5$	2497.24	2492.91		2492.74
50	$3s^2 3p^2_{1/2} 3p^4_{3/2} 3d^4_{3/2} 3d^5_{5/2} 4f_{7/2}$	$^1F^o_3$	2497.69	2493.62		2493.44
51	$3s^2 3p^2_{1/2} 3p^4_{3/2} 3d^4_{3/2} 3d^5_{5/2} 4f_{7/2}$	$^3D^o_1$	2514.68	2510.37	2513.93	2509.80
52	$3s^2 3p^2_{1/2} 3p^4_{3/2} 3d^3_{3/2} 3d^6_{5/2} 4f_{5/2}$	$^3H^o_4$	2574.63	2568.72		2568.83
53	$3s^2 3p^2_{1/2} 3p^4_{3/2} 3d^3_{3/2} 3d^6_{5/2} 4f_{5/2}$	$^1D^o_2$	2576.55	2570.87		2571.00
54	$3s^2 3p^2_{1/2} 3p^4_{3/2} 3d^3_{3/2} 3d^6_{5/2} 4f_{7/2}$	$^3D^o_2$	2581.79	2575.87		2575.96
55	$3s^2 3p^2_{1/2} 3p^4_{3/2} 3d^3_{3/2} 3d^6_{5/2} 4f_{5/2}$	$^3G^o_3$	2582.60	2576.92		2577.00
56	$3s^2 3p^2_{1/2} 3p^4_{3/2} 3d^3_{3/2} 3d^6_{5/2} 4f_{7/2}$	$^3H^o_5$	2585.02	2578.70		2578.74
57	$3s^2 3p^2_{1/2} 3p^4_{3/2} 3d^3_{3/2} 3d^6_{5/2} 4f_{7/2}$	$^3F^o_3$	2588.34	2582.28		2582.32
58	$3s^2 3p^2_{1/2} 3p^4_{3/2} 3d^3_{3/2} 3d^6_{5/2} 4f_{7/2}$	$^3G^o_4$	2589.92	2583.78		2583.81
59	$3s^2 3p^2_{1/2} 3p^4_{3/2} 3d^3_{3/2} 3d^6_{5/2} 4f_{5/2}$	$^1P^o_1$	2606.07	2599.61		2598.44
60	$3s^2 3p^2_{1/2} 3p^3_{3/2} 3d^4_{3/2} 3d^6_{5/2} 4p_{3/2}$	$^3D^e_3$	2631.18	2625.71		2625.64
61	$3s^2 3p^2_{1/2} 3p^3_{3/2} 3d^4_{3/2} 3d^6_{5/2} 4p_{3/2}$	$^1P^e_1$	2631.24	2625.85		2625.79
62	$3s^2 3p^2_{1/2} 3p^3_{3/2} 3d^4_{3/2} 3d^6_{5/2} 4p_{3/2}$	$^3P^e_2$	2636.74	2631.45		2631.50
63	$3s^2 3p^2_{1/2} 3p^3_{3/2} 3d^4_{3/2} 3d^6_{5/2} 4p_{3/2}$	$^1S^e_0$	2658.88	2654.10		2653.89
64	$3s^2 3p^2_{1/2} 3p^3_{3/2} 3d^4_{3/2} 3d^6_{5/2} 4d_{3/2}$	$^3P^o_0$	2788.46	2782.27		2781.92
65	$3s^2 3p^2_{1/2} 3p^3_{3/2} 3d^4_{3/2} 3d^6_{5/2} 4d_{3/2}$	$^3P^o_1$	2794.79	2788.46		2788.11
66	$3s^2 3p^2_{1/2} 3p^3_{3/2} 3d^4_{3/2} 3d^6_{5/2} 4d_{3/2}$	$^3F^o_3$	2797.54	2791.48		2790.75
67	$3s^2 3p^2_{1/2} 3p^3_{3/2} 3d^4_{3/2} 3d^6_{5/2} 4d_{3/2}$	$^3D^o_2$	2800.82	2794.99		2794.28
68	$3s^2 3p^1_{1/2} 3p^4_{3/2} 3d^4_{3/2} 3d^6_{5/2} 4s$	$^3P^o_0$	2808.42	2800.47		2801.60
69	$3s^2 3p^1_{1/2} 3p^4_{3/2} 3d^4_{3/2} 3d^6_{5/2} 4s$	$^3P^o_1$	2808.48	2800.31		2801.52
70	$3s^2 3p^2_{1/2} 3p^3_{3/2} 3d^4_{3/2} 3d^6_{5/2} 4d_{5/2}$	$^3F^o_4$	2827.98	2821.24		2820.47
71	$3s^2 3p^2_{1/2} 3p^3_{3/2} 3d^4_{3/2} 3d^6_{5/2} 4d_{5/2}$	$^1D^o_2$	2830.01	2823.50	2829.34	2822.78
72	$3s^2 3p^2_{1/2} 3p^3_{3/2} 3d^4_{3/2} 3d^6_{5/2} 4d_{5/2}$	$^1P^o_1$	2831.14	2824.36		2823.76
73	$3s^2 3p^2_{1/2} 3p^3_{3/2} 3d^4_{3/2} 3d^6_{5/2} 4d_{5/2}$	$^3D^o_3$	2833.57	2827.01		2826.34
74	$3s^2 3p^1_{1/2} 3p^4_{3/2} 3d^4_{3/2} 3d^6_{5/2} 4p_{1/2}$	$^3D^e_1$	2915.18	2906.53		2907.03
75	$3s^2 3p^1_{1/2} 3p^4_{3/2} 3d^4_{3/2} 3d^6_{5/2} 4p_{1/2}$	$^3P^e_0$	2933.12	2925.01		2924.79
76	$3s^2 3p^2_{1/2} 3p^3_{3/2} 3d^4_{3/2} 3d^6_{5/2} 4f_{5/2}$	$^3D^e_1$	2994.41	2987.57		2986.28
77	$3s^2 3p^2_{1/2} 3p^3_{3/2} 3d^4_{3/2} 3d^6_{5/2} 4f_{5/2}$	$^3D^e_2$	3000.22	2993.11		2991.89
78	$3s^2 3p^2_{1/2} 3p^3_{3/2} 3d^4_{3/2} 3d^6_{5/2} 4f_{5/2}$	$^3G^e_4$	3001.22	2993.86		2992.80
79	$3s^2 3p^2_{1/2} 3p^3_{3/2} 3d^4_{3/2} 3d^6_{5/2} 4f_{5/2}$	$^3F^e_3$	3005.43	2998.33		2997.24
80	$3s^2 3p^2_{1/2} 3p^3_{3/2} 3d^4_{3/2} 3d^6_{5/2} 4f_{7/2}$	$^3G^e_5$	3007.39	2999.58		2998.54
81	$3s^2 3p^2_{1/2} 3p^3_{3/2} 3d^4_{3/2} 3d^6_{5/2} 4f_{7/2}$	$^1F^e_3$	3011.62	3004.10		3002.99
82	$3s^2 3p^2_{1/2} 3p^3_{3/2} 3d^4_{3/2} 3d^6_{5/2} 4f_{7/2}$	$^3F^e_4$	3016.01	3008.45		3007.41
83	$3s^2 3p^2_{1/2} 3p^3_{3/2} 3d^4_{3/2} 3d^6_{5/2} 4f_{7/2}$	$^1D^e_2$	3019.57	3012.22	3015.40	3011.10
84	$3s^2 3p^1_{1/2} 3p^4_{3/2} 3d^4_{3/2} 3d^6_{5/2} 4p_{3/2}$	$^3P^e_1$	3055.70	3045.98		3046.07
85	$3s^2 3p^1_{1/2} 3p^4_{3/2} 3d^4_{3/2} 3d^6_{5/2} 4p_{3/2}$	$^3D^e_2$	3065.04	3054.85		3055.42
86	$3s^1 3p^2_{1/2} 3p^4_{3/2} 3d^4_{3/2} 3d^6_{5/2} 4s$	$^3S^e_1$	3083.43	3074.67		3073.68
87	$3s^1 3p^2_{1/2} 3p^4_{3/2} 3d^4_{3/2} 3d^6_{5/2} 4s$	$^1S^e_0$	3089.01	3080.82		3078.59
88	$3s^1 3p^2_{1/2} 3p^4_{3/2} 3d^4_{3/2} 3d^6_{5/2} 4p_{1/2}$	$^3P^o_1$	3184.34	3175.74		3173.11
89	$3s^1 3p^2_{1/2} 3p^4_{3/2} 3d^4_{3/2} 3d^6_{5/2} 4p_{1/2}$	$^3P^o_0$	3185.75	3177.56		3174.81
90	$3s^2 3p^1_{1/2} 3p^4_{3/2} 3d^4_{3/2} 3d^6_{5/2} 4d_{3/2}$	$^3F^o_2$	3228.80	3218.05		3219.28
91	$3s^2 3p^1_{1/2} 3p^4_{3/2} 3d^4_{3/2} 3d^6_{5/2} 4d_{3/2}$	$^3D^o_1$	3234.05	3223.51		3223.52
92	$3s^2 3p^1_{1/2} 3p^4_{3/2} 3d^4_{3/2} 3d^6_{5/2} 4d_{5/2}$	$^3P^o_2$	3259.08	3247.85		3247.74
93	$3s^2 3p^1_{1/2} 3p^4_{3/2} 3d^4_{3/2} 3d^6_{5/2} 4d_{5/2}$	$^3F^o_3$	3261.58	3250.11		3249.56
94	$3s^1 3p^2_{1/2} 3p^4_{3/2} 3d^4_{3/2} 3d^6_{5/2} 4p_{3/2}$	$^3P^o_2$	3334.76	3324.81		3322.41
95	$3s^1 3p^2_{1/2} 3p^4_{3/2} 3d^4_{3/2} 3d^6_{5/2} 4p_{3/2}$	$^1P^o_1$	3336.57	3326.67		3324.18
96	$3s^2 3p^1_{1/2} 3p^4_{3/2} 3d^4_{3/2} 3d^6_{5/2} 4f_{5/2}$	$^3G^e_3$	3432.67	3420.66		3420.19

Table 1. (*Continued*).

Level	State configuration	Level	GRASP1	GRASP2	Yang	Zeng
97	$3s^2 3p^1_{1/2} 3p^4_{3/2} 3d^4_{3/2} 3d^6_{5/2} 4f_{5/2}$	$^3F^e_2$	3438.25	3426.34		3425.43
98	$3s^2 3p^1_{1/2} 3p^4_{3/2} 3d^4_{3/2} 3d^6_{5/2} 4f_{7/2}$	$^3D^e_3$	3441.04	3428.74		3427.10
99	$3s^2 3p^1_{1/2} 3p^4_{3/2} 3d^4_{3/2} 3d^6_{5/2} 4f_{7/2}$	$^3G^e_4$	3443.52	3431.09		3430.54
100	$3s^1 3p^2_{1/2} 3p^4_{3/2} 3d^4_{3/2} 3d^6_{5/2} 4d_{3/2}$	$^3D^e_1$	3498.36	3488.02		3485.07
101	$3s^1 3p^2_{1/2} 3p^4_{3/2} 3d^4_{3/2} 3d^6_{5/2} 4d_{3/2}$	$^3D^e_2$	3500.00	3489.47		3486.18
102	$3s^1 3p^2_{1/2} 3p^4_{3/2} 3d^4_{3/2} 3d^6_{5/2} 4d_{5/2}$	$^3D^e_3$	3530.71	3519.53		3516.55
103	$3s^1 3p^2_{1/2} 3p^4_{3/2} 3d^4_{3/2} 3d^6_{5/2} 4d_{5/2}$	$^1D^e_2$	3531.66	3520.55		3517.56
104	$3s^1 3p^2_{1/2} 3p^4_{3/2} 3d^4_{3/2} 3d^6_{5/2} 4f_{5/2}$	$^3F^o_2$	3701.24	3689.67		3685.81
105	$3s^1 3p^2_{1/2} 3p^4_{3/2} 3d^4_{3/2} 3d^6_{5/2} 4f_{5/2}$	$^3F^o_3$	3703.05	3691.23		3687.51
106	$3s^1 3p^2_{1/2} 3p^4_{3/2} 3d^4_{3/2} 3d^6_{5/2} 4f_{7/2}$	$^3F^o_4$	3710.23	3697.99		3694.31
107	$3s^1 3p^2_{1/2} 3p^4_{3/2} 3d^4_{3/2} 3d^6_{5/2} 4f_{7/2}$	$^1F^o_3$	3715.03	3703.02		3699.33

3. Collision strengths

After generating the wavefunctions by GRASP, Ω can be calculated by using the DARC package of Norrington. In our calculations, 20 continuum orbitals per angular momentum are used, and the R-matrix boundary radius is determined to be 1.21 atomic units automatically by the code, which is chosen so that all large components have a magnitude less than 0.001. The maximum number of channels for a partial wave is 337, and the corresponding size of the Hamiltonian matrix is 6740.

To obtain converged Ω at all energies for all transitions, we have included the contribution of all partial waves with angular momentum $J \leq 41.5$. For the allowed transitions, the value of Ω is difficult to converge, especially when the incident energy is high. Therefore, a 'top-up' based on the sum rules of Burgess *et al.*[14] has been included to take account of the higher neglected partial waves.

To highlight the contributions of the resonances in our calculations, we have calculated Ω for all transitions among the first 59 levels at incident energies below 1742 Ryd, including the threshold region, which is between 136.4 Ryd and 191.5 Ryd. We have calculated about 10000 points in the threshold region to take account of the resonance effects, and 200 points in the region above threshold. Since no resonance effects exist above the threshold region, in this paper, we only list our results of total collision strengths at five incident energies of 300 Ryd, 600 Ryd, 900 Ryd, 1200 Ryd, and 1500 Ryd for the transitions from the ground level to higher excited levels in Table 2 for brevity. Comparisons are made with the results of Zeng *et al*. in detail.

Table 2. Collision strengths from the ground level to excited levels at five incident electron energies of 300 Ryd, 600 Ryd, 900 Ryd, 1200 Ryd, and 1500 Ryd for Ni-like Au.

Transition		Transition type	300 Ryd	600 Ryd	900 Ryd	1200 Ryd	1500 Ryd
I	*J*						
1	2	M_3	2.94-04	1.27-04	7.02-05	4.34-05	2.92-05
1	3	E_2	1.63-03	1.95-03	2.16-03	2.31-03	2.42-03
1	4	M_1	1.35-04	5.68-05	3.11-05	1.92-05	1.29-05
1	5	E_2	9.96-04	1.15-03	1.27-03	1.36-03	1.43-03
1	6	M_2	3.23-04	1.33-04	7.09-05	4.31-05	2.91-05
1	7	E_3	7.40-04	6.82-04	6.83-04	6.97-04	7.15-04
1	8	M_2	2.40-04	9.51-05	5.04-05	3.06-05	2.07-05
1	9	E_1	2.58-03	4.25-03	5.51-03	6.58-03	7.51-03
1	10	M_4	4.14-04	1.69-04	9.15-05	5.64-05	3.83-05
1	11	M_2	2.73-04	1.07-04	5.58-05	3.35-05	2.24-05
1	12	E_1	3.43-03	6.02-03	8.00-03	9.69-03	1.12-02
1	13	E_3	4.16-04	3.82-04	3.87-04	3.98-04	4.11-04
1	14		1.00-04	4.17-05	2.26-05	1.39-05	9.49-06
1	15	E_1	4.54-04	5.78-04	7.21-04	8.56-04	9.80-04
1	16	E_3	5.78-04	5.28-04	5.30-04	5.42-04	5.57-04
1	17	M_2	1.64-04	6.05-05	3.03-05	1.75-05	1.14-05
1	18	M_1	6.18-04	2.53-04	1.40-04	8.80-05	6.03-05
1	19	E_4	7.62-04	4.93-04	4.44-04	4.38-04	4.45-04
1	20	E_2	8.96-04	7.43-04	7.45-04	7.71-04	7.98-04
1	21	M_3	4.15-04	1.39-04	6.65-05	3.75-05	2.36-05
1	22	M_1	5.31-04	2.14-04	1.19-04	7.64-05	5.36-05
1	23	M_5	8.87-04	3.21-04	1.63-04	9.65-05	6.32-05
1	24	M_3	5.88-04	2.10-04	1.06-04	6.23-05	4.06-05

Table 2. (*Continued*).

Transition		Transition type	300 Ryd	600 Ryd	900 Ryd	1200 Ryd	1500 Ryd
I	*J*						
1	25	E_2	2.14-03	2.62-03	2.96-03	3.22-03	3.42-03
1	26	E_4	4.71-04	2.41-04	1.98-04	1.90-04	1.91-04
1	27		6.60-03	6.85-03	6.99-03	7.10-03	7.21-03
1	28	M_1	4.24-04	1.66-04	8.95-05	5.58-05	3.83-05
1	29	M_3	5.25-04	1.91-04	9.70-05	5.72-05	3.74-05
1	30	M_2	2.30-04	8.74-05	4.62-05	2.85-05	1.97-05
1	31	E_2	1.32-03	1.59-03	1.80-03	1.96-03	2.09-03
1	32	E_1	3.66-03	6.66-03	8.97-03	1.09-02	1.27-02
1	33	M_1	5.21-04	2.07-04	1.13-04	6.99-05	4.74-05
1	34	E_4	7.14-04	4.25-04	3.70-04	3.59-04	3.63-04
1	35	E_2	8.37-04	6.91-04	6.97-04	7.24-04	7.53-04
1	36	M_3	4.16-04	1.36-04	6.45-05	3.59-05	2.24-05
1	37		3.25-02	3.41-02	3.49-02	3.54-02	3.60-02
1	38		4.28-04	1.59-04	8.24-05	4.93-05	3.26-05
1	39	E_1	1.04-03	4.18-04	2.53-04	1.88-04	1.60-04
1	40	E_5	7.22-04	4.41-04	4.23-04	4.39-04	4.61-04
1	41	M_2	8.84-04	2.90-04	1.40-04	7.97-05	5.09-05
1	42	M_1	1.45-04	6.18-05	3.53-05	2.27-05	1.58-05
1	43	E_2	1.62-03	2.07-03	2.36-03	2.57-03	2.73-03
1	44	E_3	9.35-04	5.32-04	4.53-04	4.31-04	4.27-04
1	45	M_4	4.88-04	1.36-04	5.96-05	3.21-05	1.96-05
1	46	M_6	1.09-03	3.48-04	1.68-04	9.65-05	6.21-05
1	47	M_2	8.91-04	2.93-04	1.42-04	8.10-05	5.18-05
1	48	M_4	8.04-04	2.50-04	1.18-04	6.67-05	4.25-05
1	49	E_5	4.02-04	1.72-04	1.48-04	1.50-04	1.57-04
1	50	E_3	2.39-03	2.78-03	3.01-03	3.18-03	3.30-03
1	51	E_1	4.82-02	6.92-02	8.48-02	9.79-02	1.09-01
1	52	M_4	6.94-04	2.19-04	1.05-04	5.99-05	3.83-05
1	53	M_2	8.69-04	2.89-04	1.41-04	8.10-05	5.21-05
1	54	M_2	1.01-03	3.44-04	1.70-04	9.82-05	6.34-05
1	55	E_3	1.10-03	1.19-03	1.28-03	1.35-03	1.40-03
1	56	E_5	6.20-04	3.70-04	3.56-04	3.71-04	3.90-04
1	57	E_3	1.33-03	1.15-03	1.15-03	1.19-03	1.22-03
1	58	M_4	4.95-04	1.37-04	6.01-05	3.22-05	1.97-05
1	59	E_1	1.10-01	1.60-01	1.97-01	2.27-01	2.54-01

Systemic comparisons between our results of collision strengths and the data of Zeng *et al.* for all transitions from the ground level to higher excited levels are made. Since Zeng *et al.* did not tabulate their data in terms of initial electron energies but we do, we have to compare our results with their data graphically. From the systemic comparisons, we can conclude that the two sets of calculations are in excellent agreement with a difference less than 20% for most of the transitions. The transitions are not all shown in this paper since their number is too large.

We only find three kinds of typical discrepancies between our results of Ω and the data of Zeng *et al.*, and they can be described as follows. First, most of E_1 and E_2 transitions calculated by Zeng *et al.* have the problem of convergence at high electron incident energies as shown in Figs. 1(a) and 1(d), since there are no enough partial waves considered in their calculations. Second, strange trending of Ω appears for the calculations of Zeng *et al.* in three E_3 transitions (1–7, 1–13, and 1–16) as shown in Fig. 1(b). Third, for two transitions (1–27 and 1–37), our results are larger than those of Zeng *et al.* as shown in Fig. 1(c).

Above all, a good agreement between our DARC results and the DW values from Zeng *et al.* provides evidence to indicate that both of the two sets of calculations are accurate, though a few defects exist for several transitions in the calculations of Zeng *et al.*, as shown in Fig. 1.

In the resonance region, the value of collision strength Ω is shown in Figs. 2(a) and 2(b) for a forbidden transition (1–2) and an allowed transition (10-12), respectively, as an example to highlight the contribution of the resonances. From Fig. 2, we can clearly see that the resonance effects are important for both forbidden and allowed transitions in our calculations of Ni-like Au and the existence of the resonances will influence the effective collision strengths and the rate coefficients.

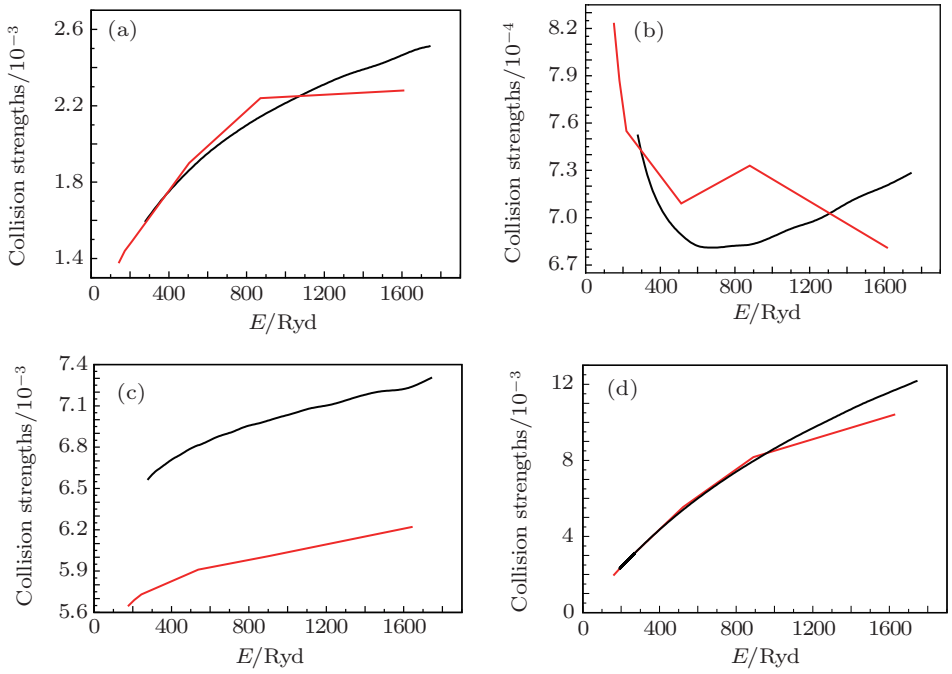


Fig. 1. (color online) Comparison of our DARC (black line) and Zeng *et al.*'s DW (red line) Ω for (a) transition 1–3 ($3s^23p^63d^{10}\ {}^1S^e_0$–$3s^23p^63d^94s\ {}^1D^e_2$), (b) transition 1–7 ($3s^23p^63d^{10}\ {}^1S^e_0$–$3s^23p^63d^94p\ {}^3F^o_3$), (c) transition 1–27 ($3s^23p^63d^{10}\ {}^1S^e_0$–$3s^23p^63d^94d\ {}^3P^e_0$), and (d) transition 1–12 ($3s^23p^63d^{10}\ {}^1S^e_0$–$3s^23p^63d^94p\ {}^1P^o_1$).

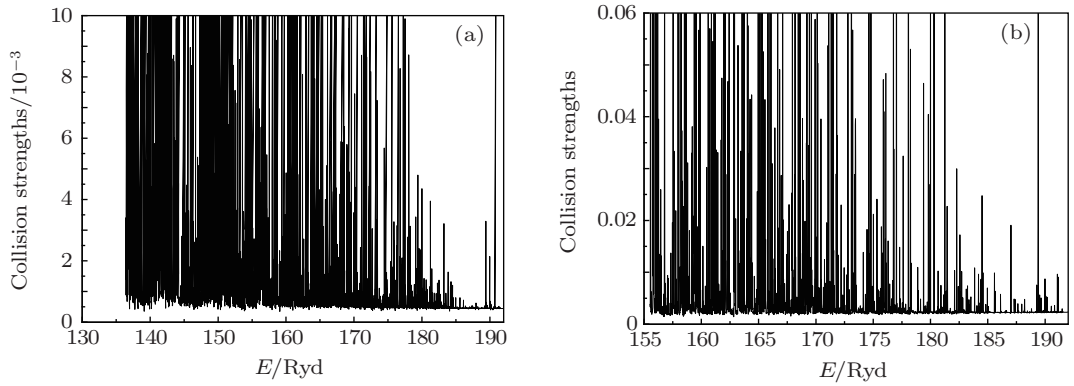


Fig. 2. (color online) (a) The Ω in the resonance region for (a) transition 1–2 (forbidden transition $3s^23p^63d^{10}\ {}^1S^e_0$–$3s^23p^63d^94s\ {}^3D^e_3$) and (b) transition 1–12 (allowed transition $3s^23p^63d^{10}\ {}^1S^e_0$–$3s^23p^63d^94p\ {}^1P^o_1$).

4. Effective collision strengths

The effective collision strengths are defined as the averaging collision strengths over a Maxwellian velocity distribution. The equation is

$$\gamma(T_e) = \int_0^\infty \Omega(E) \exp\left(-\frac{E_j}{kT_e}\right) \mathrm{d}(E_j/kT_e), \qquad (1)$$

where k is the Boltzmann constant, T_e is the electron temperature in units of K, and E_j is the electron energy with respect to the final state. Once the value of γ is known, the corresponding results for excitation $q(i,j)$ and de-excitation $q(j,i)$ rates (in units of $\mathrm{cm}^3\cdot\mathrm{s}^{-1}$) can be easily determined by

$$q(i,j) = \frac{8.63\times10^{-6}}{\omega_i T_e^{1/2}} \gamma(T_e) \exp\left(\frac{E_{ij}}{kT_e}\right), \qquad (2)$$

$$q(j,i) = \frac{8.63\times10^{-6}}{\omega_j T_e^{1/2}} \gamma(T_e), \qquad (3)$$

where ω_i and ω_j are the statistical weights of the initial (i) and the final (j) states, respectively, and E_{ij} is the transition energy.

From Eq. (1) and Fig. 2, we can see that the resonance effects have a strong influence on γ, especially when the electron temperature is low. A trapezoidal integration code is written for the calculation of γ in this paper.

Then systemic comparisons of the effective collision strengths between our results and the data of Zeng *et al.* for all transitions from the ground level to higher excited levels are made. For transitions below 1–36, our results of γ are typically several times larger than those of Zeng *et al.*, particularly at the lower end of the temperature range, as shown in Figs. 3(a) and

3(c). It is because strong resonances exist for these transitions. However, for transitions above 1–36, the two sets of calculations of γ are in good agreement with a difference of less than 20%, an example is shown in Fig. 3(b). This is because these transitions do not include many resonances.

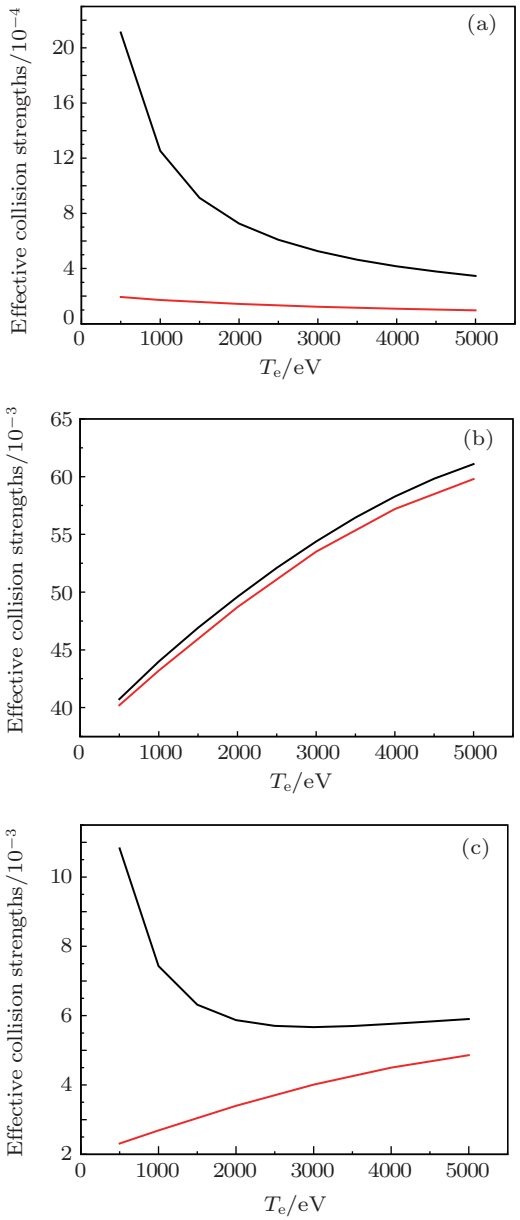


Fig. 3. (color online) Comparison of effective collision strengths of our DARC (black line) and Zeng *et al.*'s DW (red line) for (a) transition 1–17 ($3s^23p^63d^{10}$ $^1S^e_0$–$3s^23p^63d^94p$ $^3D^o_2$), (b) transition 1–51 ($3s^23p3d^{10}$ $^1S^e_0$–$3s^23p^63d^94f$ $^3D^o_1$), and (c) transition 1–12 ($3s^23p^63d^{10}$ $^1S^e_0$–$3s^23p^63d^94p$ $^1P^o_1$).

Above all, due to the resonances considered in our calculations for the effective collision strengths γ, our results of γ are typically several times larger than those of Zeng *et al.*, though the collision strengths Ω of the two sets of calculations are in good agreement for most transitions.

5. Conclusion

We have calculated the energy levels among the 107 fine-structure levels for Ni-like Au. Comparisons are made with other available theoretical results, and an excellent agreement with a difference of less than 0.2% is found. In addition, comparisons of collision strengths and effective collision strengths are also made with the DW results of Zeng *et al.* We find that the two sets of calculations for the collision strengths are in good agreement for the majority of the transitions considered. However, for the effective collision strengths, our results are generally several times larger than those of Zeng *et al*., since the contributions of the resonances are considered in our Dirac R-matrix calculations. Above all, our results are a good supplement for the atomic data of Ni-like Au.

Acknowledgments

We wish to thank Dr Patrick Norrington for providing the GRASP and DARC packages and N. R. Badnell for providing us the PSTGF package to deal with the outer region.

References

[1] Foord M E, Glenzer S H, Thoe R S, Wong K L, Fournier K B, Wilson B G and Springer P T 2000 *Phys. Rev. Lett.* **85** 992
[2] Glenzer S H, Fournier K B, Wilson B G, Lee R W and Suter L J 2001 *Phys. Rev. Lett.* **87** 045002
[3] May M J, Fournier K B, Beiersdorfer P, Chen H and Wong K L 2003 *Phys. Rev. E* **68** 036402
[4] Wong K L, May M J, Beiersdorfer P, Fournier K B, Wilson B, Brown G V, Springer P, Neill P A and Harris C L 2003 *Phys. Rev. Lett.* **90** 235001
[5] Honda K, Mima K and Koike F 1997 *Phys. Rev. E* **55** 4594
[6] Xie L Y, Dong C Z and Jiang J 2008 *Acta Phys. Sin.* **57** 2888 (in Chinese)
[7] Zhang H L and Sampson D H 1991 *Atomic Data and Nuclear Data Tables* **48** 91
[8] Zeng J L, Zhao G and Yuan J M 2007 *Atomic Data and Nuclear Data Tables* **93** 199
[9] Yang N X, Dong C Z and Jiang J 2009 *Chin. Phys. Lett.* **26** 053401
[10] Gu M F 2004 *Phys. Rev. A* **70** 062704
[11] Zhang H L and Pradhan A K 1997 *Astron. Astrophys. Suppl. Ser.* **123** 575
[12] Dyall K G, Grant I P, Johnson C T, Parpia F A and Plummer E P 1989 *Comput. Phys. Commun.* **55** 425
[13] Norrington P H and Grant I P 1987 *J. Phys. B: At. Mol. Opt. Phys.* **20** 4869
[14] Burgess A and Sheorey V B 1974 *J. Phys. B: At. Mol. Opt. Phys.* **7** 2403